Supplementary Material

A. Winter meteorological condition measurements at the AWS

Over the study period, meteorological records indicate that precipitation is associated most of the time with strong winds (between 10 and 15 m s^{-1}) generally coming from WNW, i.e., through the Col du Midi pass. Note that westerly disturbances are a classical weather pattern of the region.

Taking a close look, two main precipitation events can be observed during SP3. One during the period 21 February – 4 March, associated with a 300° direction (WNW) wind, with strong values, especially from 1 March when the wind speed was greater than 15 m s^{-1} (Figure S1). The second event, from 25 March to 1 April, is also associated with a strong WNW wind speed. However, just after the precipitation event (i.e., after 1 April 2015), the area was exposed to an ESE wind reaching 10 to 15 m s^{-1}. The significant snow erosion (0.45 m) recorded at the AWS just after the precipitation event (i.e., at the end of March 2015) demonstrates the impact of the wind on the snow distribution just after the event, over a short time period (i.e., a few hours).

During SP4, several snowfall events occurred. The main one was a 15-day precipitation event from 25 April to 9 May, associated with WNW wind speeds reaching 20 m s^{-1}. Three smaller events followed this one. The first was a 4-day event (from 13 to 16 May), also associated with strong WNW winds. The two others were 3-day events associated with lower wind speeds (5 to 10 m s^{-1}), coming from ESE (110°). In addition, higher temperatures, closer to 0°C or higher (as for instance in mid-May) were recorded over this period.

Measurements performed at the AWS during SP5 indicate small decreases in snow depth (Figure S2d), associated with temperatures close or even above 0°C, suggesting snowmelt events. Therefore, this period is not considered as the winter period for the rest of the study.

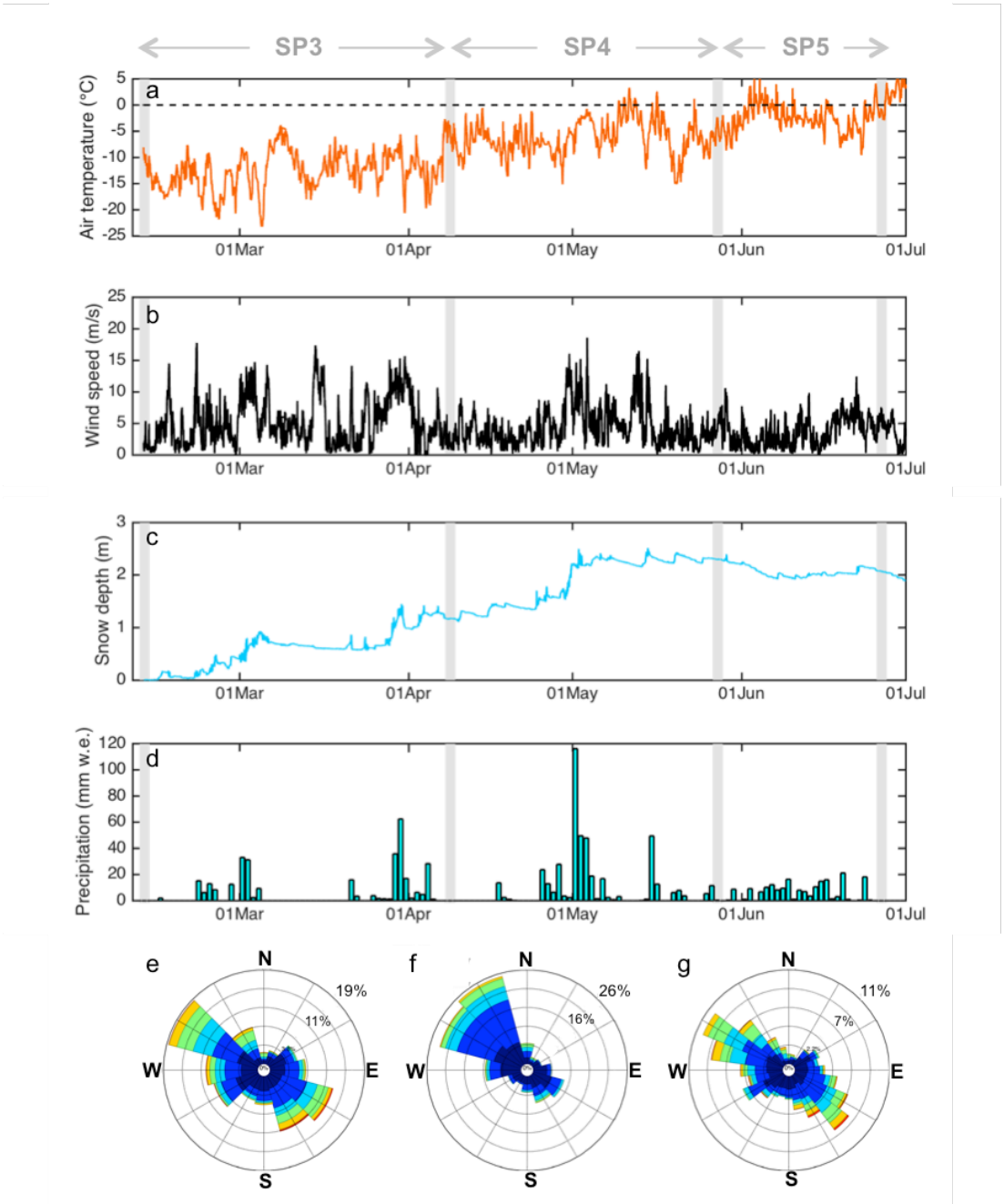

Figure S1. Hourly AWS measurements of (a) air temperature, (b) wind speed and (c) snow depth measured continuously with the SR50 over the winter period (from 11 February (installation of the AWS), until 1 July 2015). (d) Daily precipitation from SAFRAN reanalysis. Gray lines represent the date of each scan over the winter period used to delimit the sub-periods. (e), (f) and (g) show the wind roses for the three sub-periods SP3, SP4 and SP5, respectively.

B. Surface mass balance over the winter period and *Sx* index

B.1 *Sx* index calculation

To evaluate and understand the spatial variability of the surface mass balance over the winter period and the differences between each sub-period, the surface mass balance maps were compared to the wind-sheltering index of the terrain (*Sx*, Winstral and others, 2002). *Sx* was computed using equations (*S1*) and (*S2*). First it was computed for a grid point (xi, yi) (Eq. *S1*) where *A* is the azimuth of the search direction and *dmax* the search distance. Second, the *Sx* value was averaged over several azimuth values *A* across an upwind window (*A1, A2*) around a prevailing wind direction *A* (Eq. *S2*).

$$Sx_{A,dmax}\left(x_j, y_j\right) = \left(tan^{-1}\left\{elev(x_i, y_i) - elev(x_j, y_j)\ \sqrt{(x_i - x_j)^2 + (y_i - y_j)^2}\ \right\}\right) \quad (S1)$$

$$\underline{Sx}_{\underline{A},dmax}\left(x_j, y_j\right) = \frac{1}{N}\sum_{A_1}^{A_2} Sx_{A,dmax}\left(x_j, y_j\right) \quad (S2)$$

For a main wind direction, this index corresponds to the maximum upwind slope parameter and provides information on the sheltering and exposure of each individual cell at different distances. Negative *Sx* values indicated exposure relative to the shelter-defining pixel (i.e., the cell of interest was higher than the shelter-defining pixel, Winstral and Marks, 2002). Therefore, it gives a simple but reasonable representation of the local wind flow fields and therefore of the redistribution of snow by wind (e.g., Winstral and Marks, 2002; Winstral and others, 2002; Revuelto and others, 2014).

The *Sx* index was calculated over the study area based on the 1 m DEM, for all wind directions (with an interval of 10°) and for maximum distances ranging from 20 m to 1000 m. Then the *Sx* computed for each grid cell was compared to the surface mass balance maps.

B.2 Results

The *Sx* index computed for each grid cell was compared to the surface mass balance maps for each period and sub-period.

Regarding the sub-periods, as no wind direction measurements are available for SP1 and SP2, the *Sx* maps with the highest correlation between the surface mass balance over the winter period and the *Sx* index (i.e., best wind direction and distance) are shown (Figure S2 e,f). Correlations are significant, demonstrating a strong wind influence on the spatial distribution, but with different main wind directions depending on the period (i.e., 230° and 300° for SP1 and SP2, respectively). Nevertheless, the absence of meteorological records over these sub-periods prevents any meaningful interpretation of the relationship between the *Sx* index and the wind measurements for these two sub-periods.

For SP3 and SP4, the *Sx* map with the main measured wind direction and the distance with the highest correlation are represented (Figure S1 g,h), but the correlations are poor and not significant. The highest and most significant correlations are found with a main wind direction influence of 240° for SP3 (Figure S1 k) and 110° for SP4 (Figure S1 l), which does not match the observed wind direction. For SP3, this disagreement can be explained by a snow distribution influenced by two opposite wind directions: the NWN

wind during the snow falls, followed by a period dominated by ESE wind as mentioned in section A. Therefore, the redistribution of the snow cover just after the precipitation event decreases the correlation as it does not correspond to the *Sx* index characteristics. Regarding SP4, the best correlation is found for a main wind direction of 110°, which leads to a relatively homogenous map of the *Sx* in agreement with the homogeneous surface mass balance map for the same sub-period (Figure S2 d,h). Nevertheless, the surface mass balance homogeneity can be related to different events such as different wind direction influences during and after the snowfall and snowmelt events (section A).

For each period over the winter season (P1, P2, P3 and P4), the surface mass balance maps (Figures 5 b,c,d,e) are also compared to the *Sx* index maps with a wind direction of 300° (Figure S2 f), corresponding to the main wind direction measured over the entire period of measurements (i.e., February to October). The highest correlations are found for a distance of 100 m and R^2 is equal to 0.07, 0.39, 0.30 and 0.30 for P1 to P4 respectively. However, the best correlations are found for the *Sx* map corresponding to a maximum distance of 200 m and a main wind influence of 240° (Figure S2 e) where R^2 is equal to 0.74, 0.70, 0.57 and 0.52 for P1 to P4, respectively. Here again, this wind direction does not match the observations, neither for the main direction of the strongest event, nor for the main direction above a threshold of 10 m s^{-1}. It could be seen as a compromise between different wind directions observed at the study site. Indeed, as previously mentioned, the study site received several snowfalls during the winter affected by different wind directions, sometimes changing during the event and just after the snowfall. Such processes are hard to represent by such indexes.

Therefore, these results suggest that the *Sx* index should be used with caution over a time period with different snowfalls influenced by different wind directions. The *Sx* is probably better suited to explaining spatial variability of the snow depth just after a snowfall influenced by a single wind direction during and just after the snowfall. In any case, it should be used with caution over large time periods encompassing several events that include contrasting wind regimes.

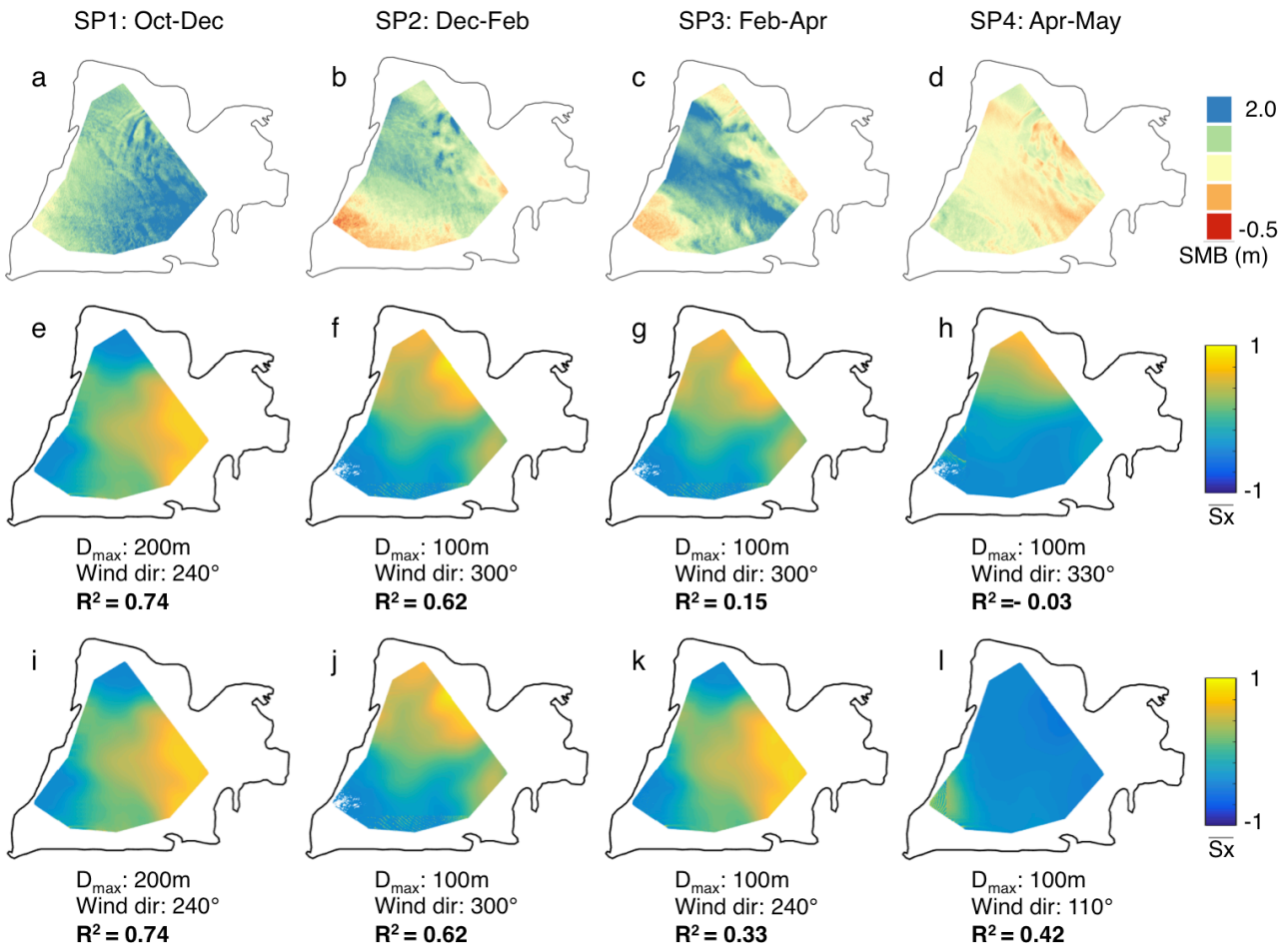

Figure S2. Surface mass balance (first row) and Sx (second and third rows) maps for the four winter sub-periods. Second row (e to h) corresponds to the best correlations for the maximum distance (D_{max}) and the main wind direction (Wind dir.). Third row (i to l) indicates the best correlations found considering all the maximum distance and wind direction possibilities.

C. DEMs differences

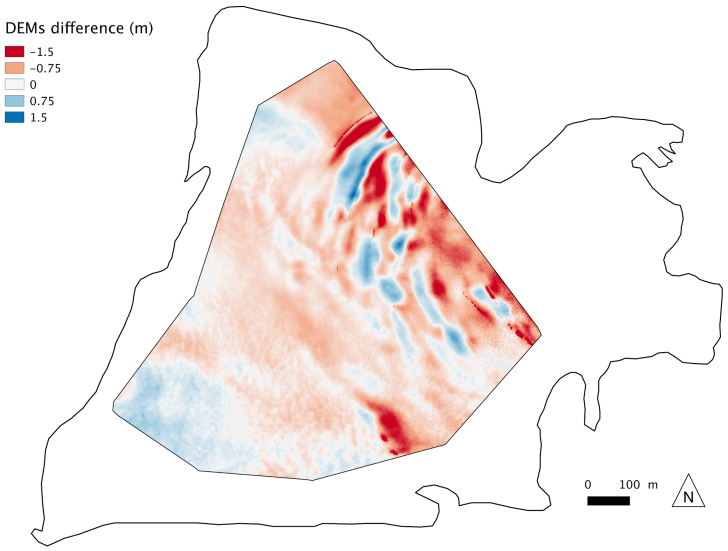

Figure S3. DEMs difference between October 2014 and October 2015. Negative values indicate a lowering of the surface.